International Journal of Advanced Research in Engineering Technology & Science ISSN: 2349-2819
Impact Factor: 7.10
(Peer-Reviewed, Open Access, Fully Refereed International Journal)
Email: editor@ijarets.org Volume-11 Issue-9 September-2024 www.ijarets.org

NANOFLUIDS AND METAL OXIDES: A BREAKTHROUGH IN THERMAL MANAGEMENT FOR LITHIUM-ION BATTERIES

Sunil Meena

Associate Professor Physics

Government College Bundi (Rajasthan)

ABSTRACT

Battery thermal management systems are excellent for cooling battery packages because of their increased power density. This is because the maximum temperature has a substantial impact on the energy storage, durability, life cycle, and efficiency of the battery. Furthermore, in order to keep the temperature within the necessary range, it is vital to select a suitable cooling technique for the battery module of an electric vehicle (EV). Using nanofluids that are flowing through the corrugated mini-channel of the electric vehicle battery cooling module, this study proposes a computational analytical technique that can be used to describe the temperature distribution and pressure drop. Four hundred forty-four lithium-ion cell batteries of the 18650 type are included in the electric vehicle battery modules. Upon investigation, it has been discovered that the temperature distributions are the most sensitive to the flow direction of the coolant, the mass flow rate, and the kinds of coolants. When compared to the traditional cooling module (Model I), the suggested module (Model II) with nanofluids as coolant demonstrated a 28.65% reduction in the maximum temperature. This was the best cooling performance of the proposed module. However, there is also an increase in the pressure drop. In addition, the cooling capacity of nanofluids as a coolant is demonstrated to be greater than that of water when used as a coolant. The current method that was developed as a result of this research has the potential to optimize the thermal management system of the battery for an electric car that operates within a temperature range that is suitable.

Keywords: *Nanofluids, Thermal, Batteries*

INTRODUCTION

The development of electric vehicles (EV) has received a significant amount of attention in recent years due to the fact that fossil fuels are a significant contributor to the production of greenhouse gases. The lithium-ion battery is widely recognized as the most promising source of energy among the numerous types of batteries that are now available for electric vehicles. This is mostly due to the fact that it possesses a high energy density, a long life cycle, and does not exhibit any memory effect. However, the temperature at which the battery is functioning must be kept within a particular range at all times. Because of the large internal resistance and the thermal reactions that take place within the cell, the battery generates a great amount of heat throughout the charge and discharge cycles. This heat is necessary for the battery to function properly. For this reason, the Battery Thermal Management System (BTMS) is absolutely necessary in

order to maintain the temperature of the battery within a safe range of operation levels. It is therefore a crucial responsibility to make use of effective BTMS in order to maintain the temperature of lithium-ion batteries in the range of 25–50 degrees Celsius while they are in operation. Generally speaking, the approaches that are available in the literature for thermal management of batteries may be broken down into three primary categories: active, passive, and hybrid, which is a combination of active and passive systems. When it comes to active ways, energy is utilized directly for the purpose of cooling. One example of this is the operation of cooling systems that utilize forced convection airflow. In passive techniques, cooling is accomplished without the need of any external energy. These methods include heat transmission through heat pipes, heat transfer through natural convection, and heat management through the utilization of phase change material (PCM). For the purpose of thermal management of battery packs, Huang et al. conducted an experimental study to assess the performance of a combined PCM/heat pipe technique (air/liquid cooled system). In order to solve for temperature, power consumption, and operating conditions within the cell, Park and Jung created a one-dimensional thermal model of a cylindrical battery using the finite difference approach. The BTMS analysis that Park has developed offers a numerical model that may be used to measure either air-based or liquid-based models. Based on the numerical analysis, it has been determined that a battery module that is both slender and has a short space between its cells is optimal for the liquid-based battery management system (BTMS). They also reported that the BTMS that is based on air consumes a greater amount of energy than the BTMS that is based on liquid. Additionally, Mahamud and Park presented a unique approach for thermal control of batteries by employing a reciprocating airflow for lithium-ion cylinders (LiMn2O4/C) by means of a two-dimensional computational fluid dynamics model. For a reciprocation time of 120 seconds, their numerical results demonstrate that the reciprocating current has the potential to lower the temperature differential between the cells by about 4 degrees Celsius and also the maximum temperature of the cells by up to 1.5 degrees Celsius. Chen et al. have optimized the manner in which battery cell distance distribution is distributed for BTMS parallel cooling. During the air-cooling process, the distance between the cell space and the battery pack is measured in order to optimize the effectiveness of the cooling system.

By optimizing the cell space using the suggested technique, the numerical results demonstrate that the cooling efficiency is greatly enhanced, which is a major improvement. In a later statement, Park demonstrated that the utilization of forced air-cooling is a viable alternative in the automotive industry. Due to the fact that a typical battery in electric hybrid cars is made up of several battery cells, the cooling performance is primarily influenced by the uniform distribution of airflow in the passageways. This airflow helps to extinguish the heat that is created by the battery cells. As a result of the limited thermal conductivity of air, a high flow rate is typically necessary in order to bring the temperature of the lithium-ion battery down. what is the thermal performance of coolants that are based on air for lithium-ion battery packs? They came to the conclusion that although a bigger airflow is beneficial for maintaining temperature uniformity, it also leads to an increase in power consumption, which in turn results in a decrease in the efficiency of the system.

Additional research demonstrates that it is hard to provide effective air cooling and consistent temperature distribution across the surface of the battery when it is subjected to unsuitable usage and stressful conditions, such as high-discharge and high ambient temperature (that is, the temperature is over 40 degrees Celsius). In order to increase operational safety, lengthen operating life, and minimize costs, it is vital to select the appropriate cooling mechanism for a lithium-ion (Li-ion) battery pack. This will ensure that the

temperature remains within the ideal range to maintain optimal performance. There are a number of criteria that need to be taken into consideration in order to select an appropriate cooling approach and design optimization techniques. These parameters include cost, complexity in geometry, weight, cooling effects, temperature uniformity, and parasitic load. Air-based cooling, direct liquid-based cooling, indirect liquid-based cooling, and fin cooling were the four types of cooling systems that Chen et al. investigated. In order to keep the same mean temperature value, the results demonstrate that the amount of energy that is required by an air cooling system is two to three times more than that required by other techniques. Direct liquid cooling is superior to indirect liquid cooling when it comes to heat dissipation; nevertheless, indirect liquid cooling has a lower cooling performance than this method. The performance of an indirect liquid cooling battery was evaluated by Chacko and Charmer, who stated that this method has the potential to be one of the most dependable approaches to accomplishing thermal management of the battery. provided an investigation of the relationship between numerical and experimental findings in tiny channel cold plates. According to the findings, elevating the discharge rate and operating temperature leads to an increase in the temperature of the cold plates. Consequently, a cooling-based battery thermal management system (BTMS) was developed for the 18650-battery model. The cells in a unique BTMS with liquid coolant are thermally coupled by aluminum components, and the description of this BTMS includes those elements.

the thermal management using nanofluid containing Al2O3. During this direct contact between the liquid and the cell, the heat that is created is dissipated by the ambient airflow. In light of the findings, it is clear that the novel approach has the potential to greatly lower the maximum temperature of the cell. In addition, nanofluids and metal foams have been the subject of substantial research because of their potential uses in cooling. The consistent experimental and computational results demonstrate that the thermal performance of nanofluids is greatly impacted by a large number of factors that are difficult to manage. Al2O3 is the nanoparticle that is utilized the most frequently because of the acceptable thermal and physical qualities it possesses. Nanoparticles like these are among the most cost-effective varieties that are now available on the market, and they are capable of providing outstanding performance and stability. Using the constant coefficients for the equation of PCM dynamic viscosity, two different techniques are described here. These approaches are A and B constant coefficients. Alternating current is used for aluminum alloy. Battery for BTMS a mechanism for managing thermal energy Charging rate for the C battery's According to the specific heat capacity (J/kg·K) of CF copper foam, dE/dT entropy coefficient (V/°C) of deionized carbon dioxide Expanded graphite used in EG It is a hybrid electric vehicle (HEV). heat sink type HS Heat transmission coefficient (W/m2 ·K) of convective heat transfer The thermal conductivity (W/m·K) as measured by the electrical current (A) The lithium-ion battery, or LIB Systems that use liquid-filled batteries (LfBS) Battery systems that use liquid circulation batteries pore count per inch (PPI) "P pressure" (in Pa) The heating power (W) of the phase change material made of PCM It is the Reynolds number. Electric resistance (Ω) is denoted by the symbol R. (K) temperature of the T in seconds (t) volts (V) voltage β pore density (PPI) is equal to the Q heat transfer rate (W). ε porosity (–) represent Greek symbols. Kinematic viscosity (m2 /s) and dynamic viscosity (kg/m·s) are the two types of viscosities that are measured. The thermal boundary layer thickness, denoted by δt-m, density of ρ (in kilograms per cubic meter) The concentration of ϱ volume: The subscripts for the base fluid eff effective in the inlet, the nanofluid out outlet, and the nanoparticles max maximum are as follows: To M. Applications of Thermal Engineering, Volume 180, Issue 2020, Pages 115840 2 Kiani et al. nanofluid cooling system (also known as. The cooling performance of the water nanoparticles slurry is given, with discharge rates of 2C and 4C respectively. Using nanoparticles, as demonstrated by their findings, has the potential to enhance the

performance of the BTMS. the efficiency of the cooling fluid in the BTMS that contains nanoparticles has been evaluated. It was discovered from the findings that nanofluids based on water work more effectively in terms of managing the maximum temperature and the temperature variation. The reason for this is because pure water has a higher heat conductivity than other base fluids, such as glycol, which are more commonly used. Al2O3-water, CuO-water, and SiCwater nanofluids are characterized by their thermal properties. At two distinct input velocities, 0.5 meters per second and 3 meters per second, the nanofluids were examined at concentrations ranging from 0.5 to 4%. In the instance of Al2O3-water and CuO-Water nanofluid slurries, the results indicate that the highest improvement for a volumetric fraction of nanoparticles of 4.0 percent was 11.98% and 11.36%, respectively. In the research conducted by Liu, a cooling system was numerically studied for a number of different base fluids, including water, ethylene glycol (EG), and motor oil. The nanofluid was utilized as the coolant in this system. When compared to EG and motor oil, water's impact is significantly more favorable because to the great heat conductivity it possesses. Additionally, it was noted that there was a tremendous rise in performance with the increase in the volume of nanoparticles that were suspended, while at the same time, the cost of power increased.

OBJECTIVE

1. to study on thermal management for lithium-ion batteries
2. to study on schematic diagram of the unstructured non-uniform grid system for the model

METHOD

The geometry model and the primary equations that govern it

Figure 1 depicts the cooling modules that were utilized in the numerical analysis that was conducted for this investigation. Table 1 provides more information regarding these modules. While the pressure is a constant that is shared by all of the phases, the continuity, momentum, and energy equations are broken down into their own distinct categories for each phase. In order to conduct an analysis of the problem, the Eulerian two-phase approach model is utilized. This model is employed on the basis of the assumptions involved, which include the neglect of viscous dissipation and radiation, incompressible nanofluids flow, constant characteristics, and homogenous nanofluids mixing. The nanofluids fluid flow and heat transfer characteristics that were flowing in the cooling module were characterized by the following equations:

$$\nabla(\rho_l \varphi \vec{V}_l) = 0 \quad (1)$$

$$\nabla(\rho_p \varphi_p \vec{V_p}) = 0 \quad (2)$$

$$\varphi_l + \varphi_p = 1 \quad (3)$$

$$\nabla(\rho_l \varphi_l \vec{V}_l \vec{V}_l) = \varphi_l \nabla p + \nabla(\varphi_l \mu_l (\nabla \vec{V}_l + \nabla \vec{V}_l T)) + F_d + F_{vm} \quad (4)$$

$$\nabla(\rho_p \varphi_p \vec{V}_p \vec{V}_p) = \varphi_p \nabla p + \nabla(\varphi_p \mu_p (\nabla \vec{V}_p + \nabla \vec{V}_p T)) - F_d + F_{vm} + F_{cd} \quad (5)$$

Only the drag force between the phases of the nanofluids has been considered as follows;

$$F_d = -\beta(\vec{V}_l - \vec{V}_p) \quad (6)$$

Where the friction coefficient, (β) and the drag coefficient, (Cd) are presented as the following equations;

$$\beta = \frac{3}{4} C_d \frac{\varphi_l(1-\varphi_l)}{d_p} \rho_l \left(\vec{V}_l - \vec{V}_p\right) \varphi_l^{-265} \tag{7}$$

$$C_d = \begin{cases} \frac{24}{\mathrm{Re}_p}\left(1 + 0.15\mathrm{Re}_p^{0.687}\right) & \mathrm{Re}_p \langle 1000 \\ 0.44 & \mathrm{Re}_p \rangle 1000 \end{cases} \tag{8}$$

Where

$$\mathrm{Re}_p = \frac{\varphi_l \rho_l \left|\vec{V}_l - \vec{V}_p\right| d_p}{\mu_l} \tag{9}$$

Based on the Eulerian two-phase turbulent model approach model, the energy equation can be written as follows;

$$\nabla\left(\rho_l \varphi_l C_{p,l} T_l \vec{V}_l\right) = \nabla\left(\varphi_l k_l \nabla T_l\right) - h_v\left(T_l - T_p\right) \tag{10}$$

$$\nabla\left(\rho_p \varphi_p C_{p,p} T_p \vec{V}_p\right) = \nabla\left(\varphi_p k_p \nabla T_p\right) - h_v\left(T_l - T_p\right) \tag{11}$$

The mono-dispersed spherical particles, (hv) and the fluid-particle heat transfer coefficient, (hp) are written as.

$$h_v = \frac{6(1-\varphi_l)}{d_p} h_p \tag{12}$$

$$h_p = \left(2 + 1.1\mathrm{Re}_p^{0.6}\mathrm{Pr}^{1/3}\right)\frac{k_l}{d_p} \tag{13}$$

The effective thermal conductivities for liquid and particle phases are obtained from

$$k_l = \frac{k_{bl}}{\varphi_l}, \cdot k_p = \frac{k_{bp}}{\varphi_p} \tag{14}$$

$$k_{bl} = \left(1 - \sqrt{(1-\varphi_l)}\right) k_l \tag{15}$$

$$k_{dp} = \left(\sqrt{(1-\varphi_l)}\right)(\omega A + [1-\omega]\Gamma) k_l \tag{16}$$

$$\Gamma = \frac{2}{\left(1 - \frac{B}{A}\right)} \left\{ \frac{B(A-1)}{A\left(1 - \frac{B}{A}\right)^2} \right\} \ln\left(\frac{A}{B}\right) - \frac{(B-1)}{\left(1 - \frac{B}{A}\right)} - \frac{B+1}{2} \tag{17}$$

$$A = \frac{k_p}{k_l} \quad and \quad \omega = 7.26 \times 10^{-3}, B = 1.25\left(\frac{1-\varphi_l}{\varphi_l}\right)^{10/9} \tag{18}$$

The proposed correlations are used to determine the nanofluids physical properties are written as follows;

$$\rho_{nf} = \varphi\rho_p + (1-\varphi)\rho_w \quad (19)$$

$$(\rho C_p)_{nf} = \varphi(\rho C_p)_p + (1-\varphi)(\rho C_p)_w \quad (20)$$

$$\mu_{nf} = (1+2.5\varphi)\mu_w \quad (21)$$

$$k_{nf} = \left[\frac{k_p + 2k_w - 2\varphi(k_w - k_p)}{k_p + 2k_w + \varphi(k_w - k_p)}\right]k_w \quad (22)$$

Boundary conditions

Boundary conditions Based on the computational domain, as shown in Fig. 1, the boundary conditions of the simulation processes are as follows;

- Inlet: uniform inlet velocity and inlet temperature

- Outlet: zero press

-constant heat flux

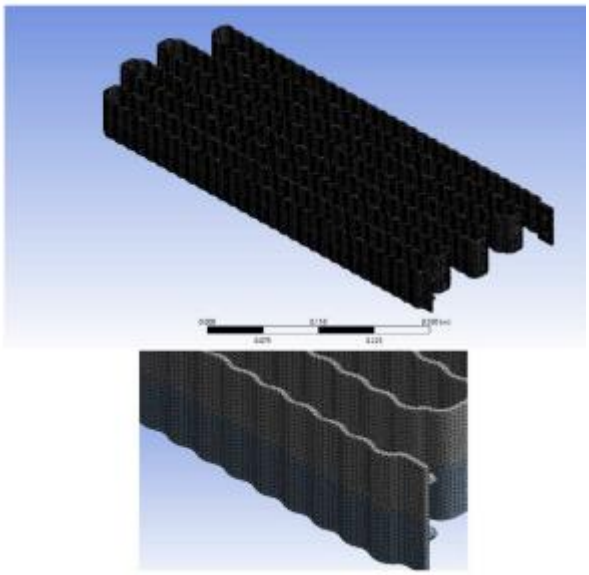

Fig. 1. Schematic diagram of the unstructured non-uniform grid system for the model.

Table 1 Grid independent check,

Models	Grid	Outlet temperature (□C)	%Difference
Model I	290,000	67.73	-
	450,000	65.98	2.66
	530,000	65.68	0.4

Model II	190,000 330,000 490,000	46.50 46.7 46.9	- 0.55 0.38
Model III	380,000 580,000 650,00	68.50 64.97 64.39	- 5.4 0.90

Simulation based on numerical data

With the help of the SIMPLEC algorithm, the second-order upwind scheme and structured uniform grid system are utilized in order to discretize the primary governing equations. This is accomplished by taking into consideration the physical problem, which is depicted in Figure 1. For the purpose of this investigation, three grid structure independence tests of the model have been carried out during the analytical process, as can be seen in Figure 2. As can be shown in Table 2, the outlet coolant temperature that was acquired from 530,000 is, according to the model I scenario, 1% more precise than the temperature that was obtained from 450,000. As a result, the grid numbers of 450,000, 330,000, and 580,000, respectively, guarantee a solution that is adequate for the model I, model II, and model III, respectively. In the current investigation, the numerical solution for the issue is the commercial application ANSYS/FLUENT. At the same time, the computer system of distributed memory (cluster) is being utilized. This system is comprised of 18 processing cores and 96 gigabytes of random access memory (RAM). The boundary conditions that are utilized in the numerical analysis are carried out under the assumption of a constant heat flow at the walls. The heat that is produced by the cylindrical lithium-ion cell batteries of type 18650 has a total of 3330 W/m2. If the residual that is summed across all of the computing nodes fulfills the condition of 10 -5, then the numerical calculation is said to have been completed.

RESULTS AND DISCUSSION

According to the literature review, as was indicated before, the majority of the previous studies have been carried out through the use of numerical analysis. Because of this, there are no experimental findings that can be used to validate the results that were anticipated for this part. Nevertheless, in order to acquire the greatest accuracy computational results at the smallest number of components, three grid-independent tests of each cooling module have been taken into consideration, as was described before. The current investigation was carried out on the continuous maximum generation of heat from a battery cell with a capacity of 12.24 watts (18650 type cylindrical battery cell, 3.4 amps, 3.6 volts). In the real operating circumstances of the battery cell, the critical working load condition is lower than the actual operating conditions. It indicates that the amount of heat produced by the battery cell is lower than the situation that was investigated in this study. It is necessary to get the surface temperature of the battery cell down to below 40 degrees Celsius and below 70 degrees Celsius for the heat created by the battery cell in order to achieve a generation heat of less than 10 watts per cell.

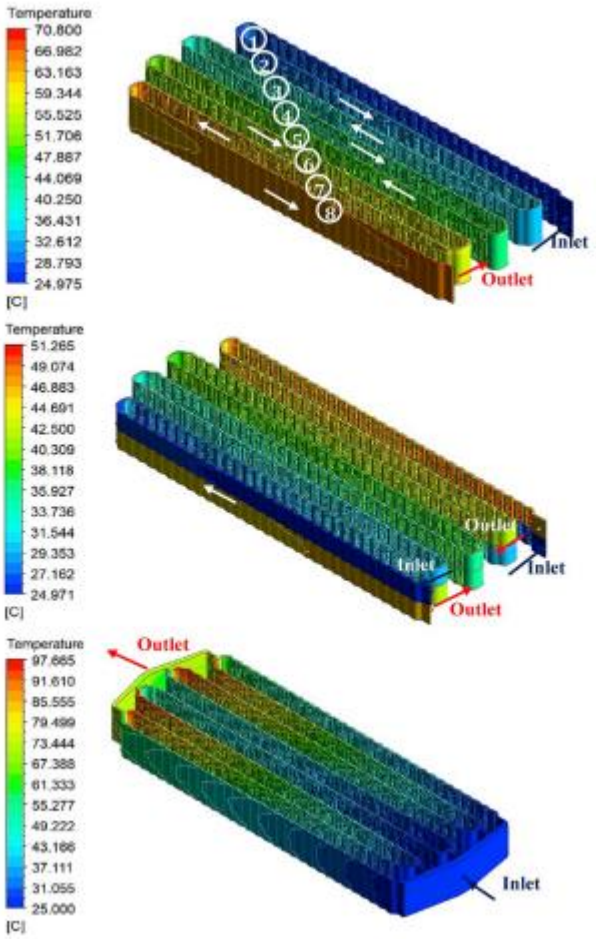

Fig. 3. Variation of temperature distribution in different models for water as working fluid.

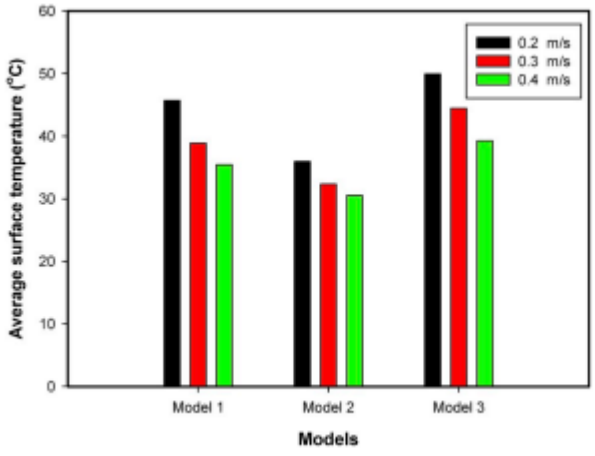

Fig. 4. Effect of coolant velocity on outlet temperature.

(20–40W per cell). During the cooling process, it was discovered that the coolant is absorbing the heat that is created from the battery cells along the corrugated mini-channel in the flow direction. This is causing the cooling capacity to decrease, which is a problem. In light of this, the temperature further downstream is invariably greater than the temperature further upstream. An increase in variance distribution will result

from cooling that is inconsistent. In light of the information presented above, model I demonstrates that the capacity of the coolant to cool the downstream is diminished. Following that, the two new cooling modules are presented and simulated in order to ascertain the maximum temperature distribution, as seen in Figure 3 (b, c). Within the context of model III, it is clear that

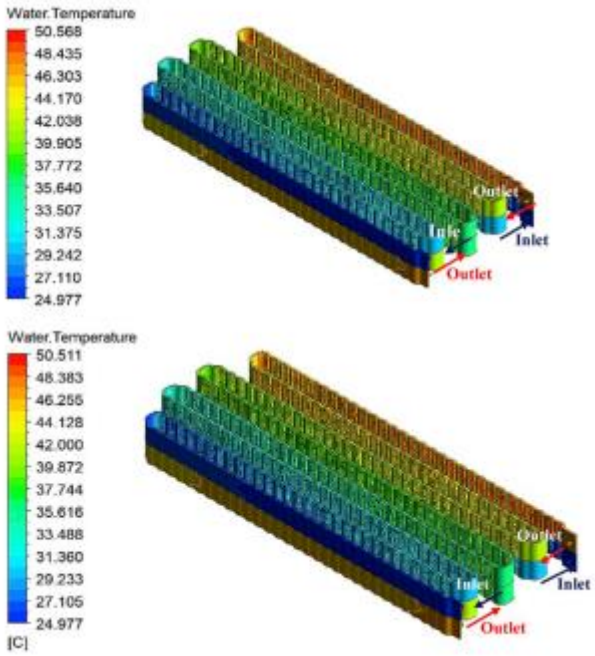

Fig. 5. Effect of nanofluids concentration on temperature distributions in the model II (0.25, 0.50% by volume).

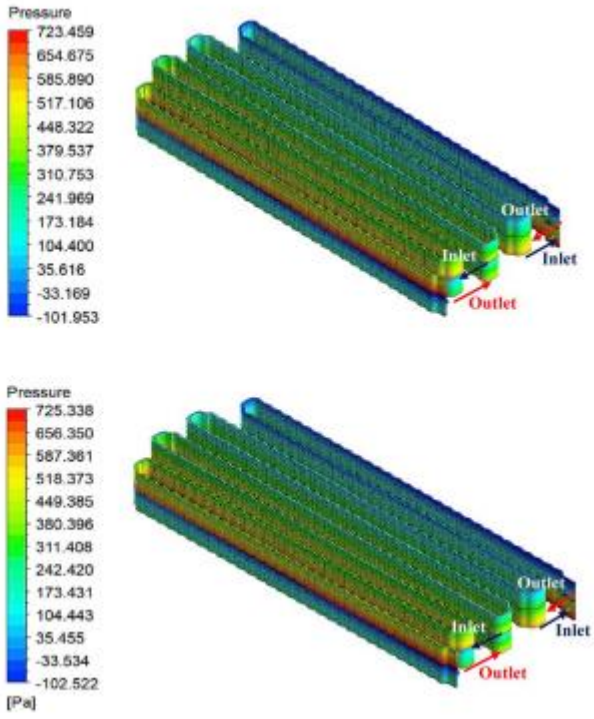

Fig. 6. Effect of nanofluids concentration on pressured distributions in the model II (0.25, 0.50% by volume).

The coolant enters the cooling module by the input manifold, then flows through the corrugated mini-channel in a distinct direction, and finally exits through the outlet manifold after it has completed its journey. It indicates that the flow rate of coolant in each mini-channel is lower than the flow rate in the other models, which is the reason why the flow rate of coolant in each mini-channel is lower than the flow rate in the other models. Similar to the model I, the cooling capacity has a tendency to decrease as the distance from the inlet port increases. This is because the coolant temperature in the downstream region is greater. Nevertheless, the coolant that is flowing into each mini-channel is not uniform, which results in the cooling capacity of coolant in each mini-channel. This is the reason why the surface battery with the maximum capacity is the lowest.

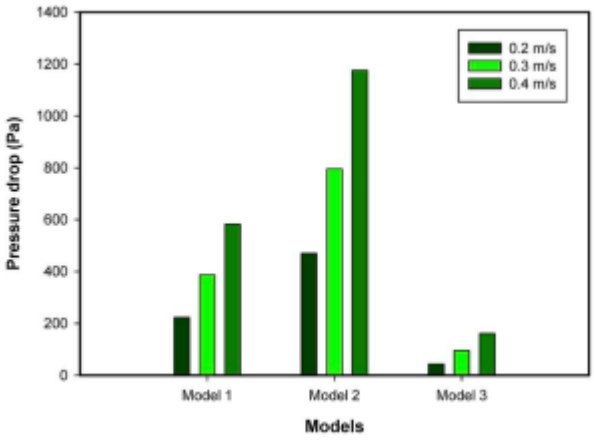

Fig. 7. Variation of pressure drop of coolants obtained from different cooling modules.

There is a temperature that may be found on the second, third, sixth, and seventh channels. The assumption that this is the case leads to the maximum surface temperature of the battery reaching 97.66 degrees Celsius, which also results in the thermal runaway. The maximum temperature of the decrement surface of the battery has not been obtained from any of the two models, as was described before. As a result, model II is presented by dividing the flow channel into upper and lower halves, as seen in Figure 1. For the purpose of cooling the battery cells, the coolant stream enters the cooling module through the upper flow channel and continues to flow alongside the cooling module the entire time. That the coolant temperature tends to be comparable to model I is something that can be observed. As a result, the maximum temperature at the downstream is lowered, and another coolant flow stream enters the lower cooling module at the opposite end, as seen in Figure 3. When compared with the general cooling module (Model I), the maximum and average surface temperatures of the battery are roughly 51.26 degrees Celsius and 38.15 degrees Celsius, respectively. These temperatures are lower by 27.59% and 20.33%, respectively. It can be observed that the surface of the battery is kept at an average temperature that falls within the required range (below 40 degrees Celsius for heat that is generated at a rate of less than 10 watts per cell). Nevertheless, there was an increase in the pressure drops that occurred across the cooling module. The influence of the coolant flow rate on the surface temperature of the battery is seen in Figure 4, which takes into account a variety of cooling modules. From the perspective of all of the cooling modules, it is clear that the temperature of the

battery's surface is sensitive to the increase in the flow rate of the coolant. The cooling capacity of coolant, which is achieved by lowering the maximum temperature of the battery surface, is, however, restricted by the fact that the flow rate of coolant may increase. Figure 5 illustrates how the concentration of nanofluids influences the highest temperature that may be reached on the surface of the battery. Within the framework of the numerical technique, the concentrations of nanofluids at 0.25% and 0.50% by volume have been carried out for the cooling module II. Titanium dioxide nanoparticles, often known as TiO2, are utilized in the analysis process for the purpose of holding nanoparticles in suspension within the base fluid. It has a substantial impact on the thermal physical characteristics of nanofluids, namely their high thermal conductivity, as well as the impact it has on the Brownian motion of nanoparticles in the base fluid. Because of this, the heat transmission capacity of nanofluids is significantly higher than that of water. As you can see in Figure 5, this indicates that the maximum temperature of the battery surface achieved by using nanofluids as a coolant is lower than the temperature achieved by using water as a coolant. As the concentration of nanofluids increases, the transferring of momentum and energy tends to rise as well. This is because of the higher surface area and the molecular collisions that occur more frequently. As a result, a larger concentration of nanofluids leads to an increase in cooling capacity, accompanied by a minor rise in the overall pressure drop throughout the cooling module, as seen in Figure 6. For each of the three different cooling schemes, the variance in pressure drop across the cooling module is depicted in Figure 7. It is clear that the pressure drop across the cooling module is sensitive to the deteriorating coolant flow rate as well as the cooling module itself. The model II cooling module has the biggest pressure drop throughout the cooling module when compared to the other three cooling modules.

CONCLUSION

It is necessary for the contemporary heat transfer development to have a high power density of the battery pack in order to spread the heat that is rejected from the battery pack in an even manner. This is necessary in order to keep the battery pack's efficiency, dependability, safety, durability, and life cycle intact. As a result of the restricted area and cooling capacity of the cooling system that is installed in the electric car, the optimal cooling performance is designed. The results of the numerical simulations of the flow of nanofluids via the corrugated mini-channel of the battery cooling modules for electric vehicles have been reported. A number of different water and nanofluid mass flow rates are shown, together with their respective impacts on the intake and flow direction of the coolant. In the beginning, the capacity to dissipate heat is increased in the upstream locations, and then it gradually decreases as one moves downstream. When compared to the standard cooling module model I, it has been discovered that the suggested model II has a maximum temperature of the battery surface temperature that is 27.59% lower than the previous model. In addition, the movement of nanoparticles that are suspended in the base fluid has a substantial impact on the cooling capacity of the coolant, which leads to a decrease in the maximum temperature of the battery when the concentration of nanofluids is increased. In the context of an electric car battery cooling module, the model that was suggested as a result of this study has the potential to successfully improve the battery thermal management system.

REFERENCES

1. H. Sun, R. Dixon, Development of cooling strategy for an air cooled lithium-ion battery Pack, J. Power Sources 272 (2014) 404–414.

2. Jarrett, Y. Kim, Influence of operating conditions on the optimum design of electric vehicle battery cooling plates, J. Power Sources 245 (2014) 644–655.
3. Q. Wang, B. Jiang, Q.F. Xue, H.L. Sun, B. Li, H.M. Zou, Y.Y. Yan, Experimental investigation on EV battery cooling and heating by heat Pipes, Appl. Therm. Eng. 88 (2015) 54–60.
4. F. Liu, F. Lan, J. Chen, Dynamic thermal characteristics of heat pipe via segmented thermal resistance model for electric vehicle battery cooling, J. Power Sources 321 (2016) 57–70.
5. L. Feng, S. Zhou, Y. Li, Y. Wang, Q. Zhao, C. Luo, G. Wang, K. Yan, Experimental investigation of thermal and strain management for lithium-ion battery pack in heat pipe cooling, J. Energy Storage 16 (2018) 84–92.
6. Q. Huang, X. Li, G. Zhang, J. Zhang, F. He, Y. Li, Experimental investigation of the thermal performance of heat pipe assisted phase change material for battery thermal management system, Appl. Therm. Eng. 7. 141 (2018) 1092–1100.
7. J. Zhao, Z. Rao, Y. Li, Thermal performance of mini-channel liquid cooled cylinder based battery thermal management for cylindrical lithium-ion power battery, Energy Convers. Manag. 103 (2015) 157–165.
8. Greco, X. Jiang, A coupled thermal and electrochemical study of lithium-ion battery cooled by paraffin/porous-graphite-matrix composite, J. Power Sources 315 (2016) 127–139.
9. R. Zhao, J. Gu, J. Liu, Optimization of a phase change material based internal cooling system for cylindrical Li-ion battery pack and a hybrid cooling design, Energy 135 (2017) 811–822.
10. D. Chen, J. Jiang, G.H. Kim, C. Yang, A. Pesaran, Comparison of different cooling methods for lithium ion battery cells, Appl. Therm. Eng. 94 (2016) 846–854.